DOI: 10.1002/cphc.200((will be filled in by the editorial staff))

Combined experimental and computational studies on the physical and chemical properties of the renewable amide, 3-acetamido-5-acetylfuran

Yi Liu,[a] Christopher N. Rowley*[a] and Francesca M. Kerton*[a]

The pK_a of 3-acetamido-5-acetylfuran (3A5AF) was predicted to be in the range 18.5 – 21.5 using the B3LYP/6-311+G(2d,p) method and several amides as references. The experimental pK_a value, 20.7, was determined via UV-Vis titrations. Its solubility was measured in methanol-modified supercritical CO_2 (mole fraction, 3.23 × 10^{-4}, cloud points 40 °C to 80 °C) and is less soluble than 5-hydroxymethylfurfural (5-HMF). Dimerization energies were calculated for 3A5AF and 5-HMF to compare hydrogen-bonding, as such interactions will affect their solubility. IR and ^{1}H NMR spectra of 3A5AF samples support the existence of intermolecular hydrogen-bonding. The HOMO, LUMO and electrostatic potential of 3A5AF were determined through MO calculations using B3LYP/6-311+G(2d,p). The $\pi - \pi^*$ transition energy (TD-DFT study) was compared with UV-Vis data. Calculated atomic charges were used in an attempt to predict the reactivity of 3A5AF. A reaction between 3A5AF and CH_3MgBr was conducted.

1. Introduction

Nowadays chemicals generated from biomass are being studied extensively because of the potential crisis surrounding the depletion of fossil fuels. Biomass can be derived from plants or animals, including lignocellulosic biomass. To date, the products obtained from biomass mainly contain C, H and O atoms.[1] The use of biomass-feedstocks containing other elements and functional groups would broaden the range of chemicals that can be derived from biomass. Therefore, the synthesis of renewable compounds containing heteroatoms is of considerable interest but remains relatively underexplored.[2] Chitin is an abundant biopolymer and can be obtained from the shells of crustaceans (i.e. fishery/food industry waste).[3] *N*-acetyl-D-glucosamine (NAG) is the monomer of chitin, and can be converted to a N-containing product, 3-acetamido-5-acetylfuran (3A5AF), through dehydration (Scheme 1). As far as we are aware, 3A5AF is the first reported nitrogen-containing product that can be obtained from the dehydration of a hexose in solution,[4] and we hope it can be a building block for a range of renewable amines and polymers in the future. Previously, 3A5AF was obtained from NAG using pyrolysis methods, but the yields were very low (2% and 0.04%).[5] In recent research, the yield of 3A5AF from NAG was increased up to 60% by the use of dimethylacetamide (DMA) as the solvent, with boric acid and sodium chloride as additives under microwave irradiation.[4] Very soon after that, another study on the dehydration of NAG in ionic liquids achieved a similar yield of 3A5AF.[6] More recently, 3A5AF has been prepared directly from chitin albeit in lower yields due to the incalcitrant nature of the biopolymer.[7] NAG has also been partially dehydrated in superheated water under autocatalytic conditions to yield Chromogen I and Chromogen III in yields of 23%.[8] As an alternative to dehydrative approaches to using this renewable aminosugar, the aerobic oxidation of NAG has been performed in water using gold nanoparticle catalysts to give *N*-acetylglucosaminic acid.[9]

To date, no studies on the chemistry of 3A5AF beyond its preparation have been reported, so this compound is awaiting further exploration in terms of its physical and chemical properties. In this paper, we endeavor to describe some important properties of 3A5AF, including its pK_a value, intermolecular interactions and electronic structure. These properties are of interest because they are fundamental to understanding the chemistry of this renewable molecule and will allow chemists to design better routes towards its isolation. For example, could supercritical carbon dioxide ($scCO_2$) be used to extract this product in an environmentally friendly way from reaction mixtures, or could acidification/basification approaches be used to separate this amide from non-*N*-containing by-products (e.g. levulinic acid, 5-hydroxymethylfurfural) in a biorefinery using shellfish waste as a feedstock? The pK_a of 3A5AF will be important in determining its reactivity in this regard. Furthermore, these data could help predict other possible reactions and optimizations to obtain desirable products.

[a] *Y. Liu, Prof. C. N. Rowley, Prof. F. M. Kerton*
Department of Chemistry
Memorial University, St. John's, NL, Canada A1C 5S7
Fax: (+1) 709 8643702
E-mail: fkerton@mun.ca, cnrowley@mun.ca

Supporting information for this article is available on the WWW under http://www.chemphyschem.org or from the author.

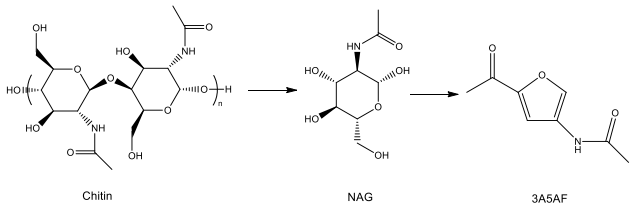

Scheme 1. Conversion of chitin to NAG and the dehydration of NAG to 3A5AF.

Computational chemistry has become very effective in predicting properties of compounds and explaining their behaviour.[10] In this way, computational work can be thought of as a complement to experimental research. In this study, we used computational calculations to predict the pK_a value and possible reaction sites within 3A5AF, and to explain the solubility performance of 3A5AF in the non-polar "green" solvent $scCO_2$.

2. Results and Discussion

2.1 pK_a Calculation and Measurement

In our study, dimethyl sulfoxide (DMSO) was chosen as the solvent because it permits a wide range of pK_a values from 0 to 30 to be determined and also allows easy comparison with other values in the scientific literature.[11] Computational investigations were performed ahead of UV-Vis titrations so that an indicator with an appropriate pK_a range could be selected.

2.1.1 Computational Studies

The pK_a of a molecule is related to the Gibbs energy of deprotonation in solution (ΔG_{soln}) by the relation pK_a = ΔG_{soln}/(RTln10). The thermodynamic cycle in Figure 1 was used, following the computational procedure of Sadlej-Sosnowska.[12] The free energy change in solution (ΔG_{soln}) is the sum of the Gibbs energy change in the gas-phase (ΔG_g) and the change in the solvation energy (ΔG_s).

From Figure 1, equations (1) to (3) are obtained as follows:

$$\Delta G_{soln} = \Delta G_g + \Delta G_s \quad (1)$$

$$\Delta G_g = G(A^-_g) + G(H^+_g) – G(HA_g) \quad (2)$$

$$\Delta G_s = \Delta G_s(A^-) + \Delta G_s(H^+) – \Delta G_s(HA) \quad (3)$$

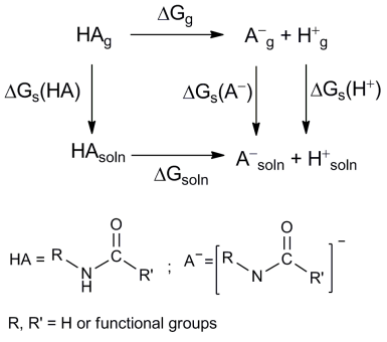

Figure 1. A thermodynamic cycle of an amide HA.

While some studies have attempted to calculate the absolute pK_a from computational data,[13] there are limitations to the accuracy of these methods due to the sensitivity of the pK_a to small errors in the calculation of ΔG_{soln} and uncertainty in the solvation energy of a proton.[12c, 14] Instead, we have calculated the pK_a of 3A5AF relative to amides with known pK_a values. Since pK_a = ΔG_{soln}/(RTln10), for two compounds the relationship pK_{a1} – pK_{a2} = (ΔG_{soln1} – ΔG_{soln2})/(RTln10) will exist. The advantage of this method is that uncertainty associated with the solvation energy of a proton is eliminated. For this method, another acid with a known pK_a value is needed. Ideally, acids with similar structures and acidities are used. During our model establishment for species in solution, the solvent effect was considered. The solvation energy is calculated from the difference between the free energy in solution and the free energy in the gas-phase. The pK_a values of a series of aromatic amides were used as references, thus several pK_a values of 3A5AF were calculated and found to be in the range of 18.5 – 21.5 (Table 1). These pK_a values are similar to those of most amides,[11] indicating that 3A5AF has a weak Brønsted acidity. The importance of solvation to the relative acidities of amides is apparent when the pK_a values calculated for solution are compared to those calculated for the gas phase. For example, with solvation taken into account, a pK_a of 18.5 was obtained using phenylacetamide as a reference, but a significantly less acidic value of 14.8 was predicted based on gas-phase calculations.

2.1.2 Experimental Measurement via UV-Vis Titration

In order to measure the pK_a of 3A5AF experimentally, an overlapping indicator method was used.[17] An acid (HIn) with a known pK_a value is used as the indicator and its conjugate anion (In^-) must give rise to a strong absorption in the UV-Vis region. The solution of the unknown acid is then added to the indicator solution, and an equilibrium will form as shown in Scheme 2.

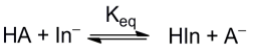

Scheme 2. The equilibrium between the indicator and the compound of interest in solution. (HA: the compound of interest; HIn: the indicator).

Table 1. pK_a(DMSO) of 3A5AF estimated computationally using the pK_a(DMSO) of amides as references and measured experimentally using UV-Vis titration.[a]

	Reference Compounds[b]	ΔG_g[c] (kJ/mol)	ΔG_s[c] (kJ/mol)	pK_a of 3A5AF[d]
Computational estimates	Phenylacetamide (21.4)	1463.48	-188.55	18.5
	Benzamide (23.4)	1499.89	-226.76	20.7
	Isonicotinamide (21.5)	1450.79	-192.23	21.4
	2-Thiophenecarboxamide (22.3)	1484.24	-222.19	21.5
	Phenoxyacetamide (23.0)	1465.85	-193.47	20.5
Experimental measurement	–	–	–	20.7 ± 0.1

[a] The Gibbs energy changes in gas-phase were calculated using G3MP2[15]; the solvation energy changes were calculated using the PCM-B3LYP/6-311+G(2d,p) method[16]. [b] The reference pK_a values were obtained from experimental data[11]. [c] Gas-phase energy changes and solvation energy

changes of the compounds with known pK_a values. [d] ΔG_g(3A5AF) = 1424.17 kJ/mol; ΔG_s(3A5AF) = -166.31 kJ/mol.

The pK_a value of HA can be calculated using equation (4), which relates this to the pK_a value of the indicator:

$$pK_a(HA) = pK_a(HIn) - \log K_{eq} = pK_a(HIn) - \log\{([HIn][A^-])/([HA][In^-])\} \quad (4)$$

In the UV-Vis spectra, a wavelength is chosen at which only the absorption of one species in the equilibrium is observed and the intensity of absorption at this wavelength is monitored as concentrations change. By recording these changes during the titration the concentration of the species can be determined using Beer's law, and using the reaction equation the concentrations of the other three species present can be calculated.

Fluorene (pK_a = 22.6) was selected as the indicator on the basis of its similar pK_a to those determined computationally for 3A5AF (Table 1). The average pK_a value of 3A5AF was 20.7 ± 0.1, after obtaining titration data in triplicate, which is within the range of the computational calculations, and is closest to the computational result obtained using benzamide as the reference, 20.7 (Table 1). This indicates that pK_a estimates provided by computation are reasonable. This value is slightly lower than the values of most amides reported in the literature,[11] but overall 3A5AF is still a very weak acid. The fact that benzamide (a primary amide) rather than phenylacetamide (a secondary amide) gave the closest computational result compared with the experimental data is a little surprising. We assumed that phenylacetamide, which has the most similar structure to 3A5AF compared with other amides employed, would give the best agreement between experiment and theory. A systematic determination of amide pK_a values using a consistent experimental method could resolve some of these discrepancies.

2.2 Solubility Measurement

2.2.1 Determination of Solubility of 3A5AF in Supercritical Carbon Dioxide Using a Phase Monitor

The phase behavior of 3A5AF in $scCO_2$ was studied using a phase monitor. A small amount of solid 3A5AF (17.5 mg) was placed in the cell and then liquid CO_2 (30 mL) was added. In neat $scCO_2$, at 60 °C and pressures up to 462 bar, the mixture in the cell was cloudy indicating incomplete dissolution. Therefore, methanol was used as a co-solvent. 3A5AF was dissolved in methanol first and the solution was injected into the cell. The mixture could be readily dissolved at all temperatures tested by increasing the pressure to certain values. The mole fraction solubility was determined to be 3.23×10^{-4}. Cloud points were observed at the following pressures (in bar) at all five temperatures: 40 °C, 263.5 ± 0.9; 50 °C, 280.1 ± 3.7; 60 °C, 304.2 ± 5.1; 70 °C, 331.8 ± 0.5; 80 °C, 351.7 ± 0.3 (Figure 2). Compared with the solubilities of several other bio-sourced molecules in $scCO_2$/methanol also determined in our group,[18] from 45 °C to 80 °C, 3A5AF is more soluble than tartaric acid, less soluble than 2,5-furandicarboxylic acid, fumaric acid, oxalacetic acid and malic acid, and has a similar solubility to succinic acid. However, it is significantly less soluble than 5-hydroxymethylfurfural (5-HMF) (Figure 3), which is the product of fructose and glucose dehydration reactions and is prepared in a similar way to 3A5AF. 5-HMF is soluble in neat $scCO_2$ and does not need a hydrogen-bonding co-solvent to dissolve in this medium. This likely indicates that the intermolecular forces between molecules of 3A5AF (solute-solute interactions) are significantly stronger in comparison to 5-HMF. For sugars and their amide derivatives, Potluri *et al.*[19] showed that acetylation increased the solubilities of these compounds in $scCO_2$ because hydrogen-bonding between solute molecules was reduced. As $scCO_2$ is a non-polar solvent and has a relatively low density,[20] only substances with weak solute-solute interactions will dissolve readily in it without an additional co-solvent. Computational studies were undertaken in order to get a more detailed understanding of the differences in strength of solute-solute interactions between 5-HMF and 3A5AF.

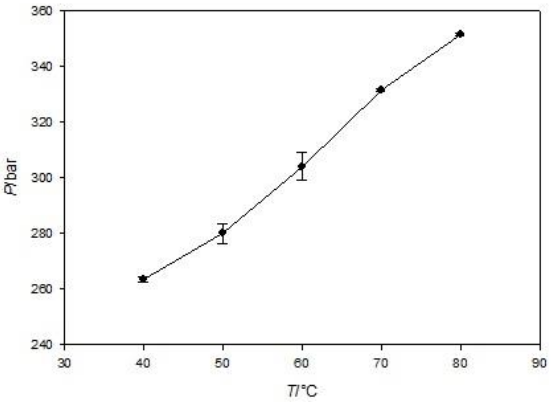

Figure 2. Temperature-pressure phase diagram for 3A5AF in $scCO_2$/methanol. Error bars: pressure ± 0.3 to 5.1 bar.

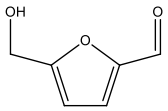

5-HMF

Figure 3. The structure of 5-hydroxymethylfurfural.

2.2.2 Calculation of Dimerization Energy

To provide some insight into why 3A5AF is immiscible in $scCO_2$ but 5-HMF, a structurally similar furan, is, we modeled the intermolecular interactions for these compounds. These calculations are based on the free energy of mixing.

$$\Delta G_{mix} = \Delta H_{mix} - T\Delta S_{mix} \quad (5)$$

From the experimental studies, for a binary mixture of $scCO_2$ and these furans, ΔG_{mix}(5-HMF) < ΔG_{mix}(3A5AF). As experimentally, the temperature range and mole ratios of solute to solvent were similar, one can assume that $T\Delta S_{mix}$(5-HMF) ≈ $T\Delta S_{mix}$(3A5AF). The differences in ΔG_{mix} (equation 5) for these 2 systems must arise from enthalpic contributions i.e. their intermolecular interactions. These intermolecular interactions favor the separation of the solute into a separate phase. Beyond the common central furan-ring motif, these molecules contain different functional groups and therefore, stronger interactions such as hydrogen-bonding will play a significant role in the different values of ΔG_{mix} between the two systems.

In order to examine this hypothesis, the Gibbs energies of dimerization (ΔG_{dimer}) of 5-HMF and 3A5AF molecules were

calculated. 5-HMF, which dimerizes through an O–H ··· O=C hydrogen bond has a ΔG_{dimer} of –10.7 kJ/mol. For 3A5AF, intermolecular hydrogen bonds can be formed between the amide N–H bond and the carbonyl of either the amide or acetyl groups (Figure 4, models 1 and 2, respectively). Dimerization energies were calculated to be –30.7 kJ/mol and –24.1 kJ/mol, respectively.

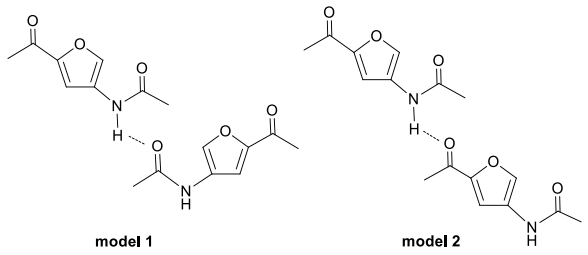

Figure 4. Schematics of the two putative hydrogen bonded 3A5AF dimers. (Dimerization energies: model 1: –24.1 kJ/mol; model 2: –30.7 kJ/mol).

The greater hydrogen bonding abilities of amides like 3A5AF in comparison to alcohols like 5-HMF is apparent in the dimerization energies. Comparing ΔG_{dimer} values, 3A5AF forms dimers more readily than 5-HMF, indicating that stronger solute-solute interactions will exist within a bulk sample of 3A5AF, and thus is less readily dissolved in $scCO_2$. It should be noted that the enthalpic contribution from such hydrogen-bonding processes is not the exclusive reason for the differences in solubility observed, but these data clearly show the presence of stronger hydrogen-bonding within 3A5AF than 5-HMF. These results indicate that useful solvent systems for future reactions of 3A5AF will require alcohols (and other "green" hydrogen-bonding solvents) or combinations of such solvents with $scCO_2$ to overcome the hydrogen bonding-tendency of the amide moiety.

2.2.3 Infrared and NMR Detection of Hydrogen-bonding in 3A5AF Molecules

In order to better prove the existence of hydrogen-bonding between 3A5AF molecules, IR spectra were obtained for both a solid sample of 3A5AF and a dilute solution (diethyl ether, Et_2O, as the solvent). The carbonyl stretching frequency ($\nu_{C=O}$) for 3A5AF was 1652.68 cm^{-1} in the solid sample and 1668.68 cm^{-1} in solution. This is a difference of 16 cm^{-1}. As the bands for $\nu_{C=O}$ of secondary amide and ketone functional groups appear in the same region, it is not possible to use IR to distinguish between the modes of intermolecular hydrogen-bonding. However, one might assume that as 3A5AF molecules are closer together in the solid-state more hydrogen-bonding will occur and this might cause a shift of $\nu_{C=O}$ towards lower frequency. In the diluted sample, interactions between 3A5AF molecules will be reduced and hydrogen-bonding between the amide proton and the ethereal oxygen atom will also decrease. For 5-HMF the $\nu_{C=O}$ is 1656.65 cm^{-1} in the solid state and 1685.47 cm^{-1} in the solution (Et_2O as the solvent). The difference is 28.8 cm^{-1}, which is larger than for 3A5AF samples. To some extent, this supports the hypothesis that stronger hydrogen-bonding exists in samples of 3A5AF than in 5-HMF as the $\nu_{C=O}$ for 3A5AF is less upon going from neat samples to diluted solutions.

NMR spectroscopy was also used to detect the hydrogen-bonding. Three NMR samples with different 3A5AF concentrations were prepared. At 298 K, as the concentration in chloroform-d ($CDCl_3$) was increased from 1.23 mg/mL to 7.35 mg/mL, δ(NH) shifted downfield from 7.18 ppm to 7.67 ppm, which is indicative of increased hydrogen-bonding within the sample.[21] Spectra were also obtained at higher temperature (323 K), and δ(NH) shifted to lower frequency, as hydrogen-bonding was disrupted by the increase in temperature. Compared with the spectra obtained at 298 K, the concentrated, 7.35 mg/mL, sample exhibited a smaller temperature dependent shift, Δ 0.06 ppm, than the dilute, 1.23 mg/mL, sample, Δ 0.13 ppm. The more concentrated sample contains more extensive hydrogen-bonding between the 3A5AF molecules, so the chemical shift varies less with changes in temperature. Finally, deuterium oxide (D_2O) was added to the samples so that deuterium exchange would occur. Qualitatively, the rate of deuterium incorporation into 3A5AF for the more concentrated samples occurred more slowly than for the dilute samples. This might also illustrate that the hydrogen-bonding is stronger in the more concentrated sample, which would inhibit the rate of deuterium exchange.

2.3 Chemical Properties of 3A5AF

2.3.1 Computational Deduction

Firstly, the energies of frontier orbitals for the geometry-optimized structure of 3A5AF were calculated by TD-DFT study. The excitation energy (ΔE) obtained was 4.278 eV, which corresponds to a wavelength of 289.83 nm. The primary component of this excitation is a π- π^* HOMO (Highest Occupied Molecular Orbital) to LUMO (Lowest Unoccupied Molecular Orbital) transition. This is in acceptable agreement with experimental data for 3A5AF, as the UV-Vis spectrum exhibits a π- π^* transition at 266.8 nm (4.650 eV). Figure 5 shows the isosurfaces of the frontier orbitals.

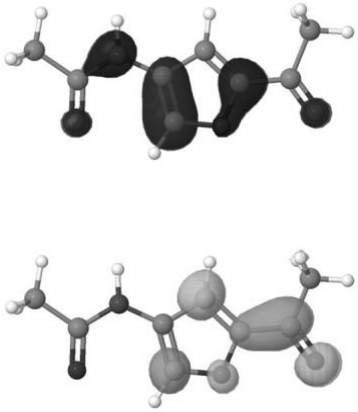

Figure 5. Isosurfaces of the HOMO (top) and LUMO (bottom) of 3A5AF. (Colour image in Supporting Information

These data were used to visualize the electrostatic potential of 3A5AF. This is affected by the electronegativity of atoms, the dipole moment and partial charges.[22] At points around the molecule, the electrostatic potential, V(r), is defined as the energy required to remove a unit point charge from a point, r, at the molecular surface.[23] Sections of the surface with a more positive electrostatic potential surface, corresponding to a net positive charge, are rendered in blue. Sections with more negative values of the electrostatic potential, corresponding to a net negative charge, are rendered in red. The colors of neutral regions range from green to yellow. The electrostatic potential map of 3A5AF is shown in the top part of Figure 6. The surface near the carbonyl

oxygens is strongly negatively charged, while the amide proton shows a blue positive charge. This is consistent with the amide-amide hydrogen bonding interactions examined in Section 2.2.2. The surface near the hydrogen on the 4 position of the furan ring also has a significantly positive electrostatic potential, indicating that this hydrogen is protic. In contrast, the electrostatic potential surface of 5-HMF (Figure 6, bottom) shows the molecule to be largely non-polar, consistent with the weaker dimerization energy of 5-HMF.

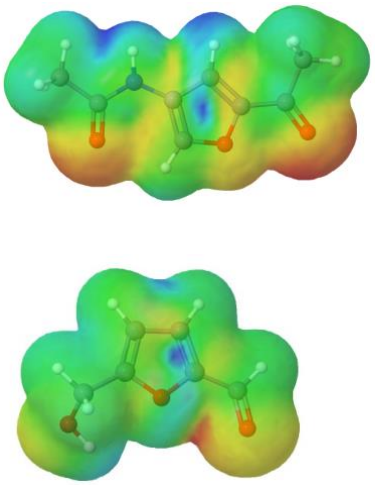

Figure 6. The electrostatic potential maps of 3A5AF and 5-HMF. (Top: 3A5AF; Bottom: 5-HMF).

In addition, the electrostatic potential (ESP) atomic partial charges of 3A5AF were calculated (Table 2). Surprisingly, the ESP charge of O15 (amide group) is more negative than that of O18 (acetyl group). This means that the amide of one 3A5AF molecule should form a strong hydrogen-bond with a neighbouring molecule. This contradicts conclusions based on the dimerization energies described in Section 2.2.2. Therefore, we believe that the steric interactions are more favorable between two 3A5AF molecules via amide-acetyl hydrogen-bonding compared with amide-amide hydrogen-bonding.

Table 2. ESP charges of several atoms in 3A5AF[a].

3A5AF structure	Code	Atom	ESP charge (e)
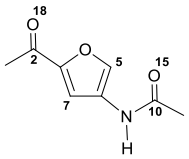	2	C	0.532
	5	C	–0.153
	7	C	–0.415
	10	C	0.791
	15	O	–0.601
	18	O	–0.511

[a] The ESP charges were calculated using B3LYP/6-311+G(2d,p) method.

2.3.2 Reaction of 3A5AF with a Methyl Grignard Reagent

The data in Table 2 suggest that C10 will react more readily with a nucleophile (e.g. Grignard reagent) than C2 due to its more positive atomic charge. However, these calculations were performed on a neutral molecule and as many nucleophiles are basic, the first equivalent of such reagents will act to deprotonate the amide group. In this study, 3A5AF was mixed with two equiv. methylmagnesium bromide (CH_3MgBr) under N_2 at room temperature for 1 h. The conditions for the reaction were chosen based on reactivity studies performed on commercially available aromatic compounds e.g. acetophenone. Upon addition of CH_3MgBr to 3A5AF, bubbles could be seen indicating the formation of methane gas as a result of deprotonation of the amide by the Grignard reagent (Scheme 3). After quenching using excess water and extraction, the reaction mixture was analyzed by GC-MS, IR spectroscopy, ^1H and ^{13}C NMR spectroscopy. As there was approximately 26% (from ^1H NMR data) unreacted 3A5AF in the mixture, the reactivity of 3A5AF towards nucleophiles is relatively low compared with an analogous reaction of acetophenone where 100% conversion was achieved under identical conditions. **1** and **1'** are possible products of a Grignard reaction with 3A5AF. Unfortunately, due to the residual 3A5AF present in the mixture, the unequivocal identification of the products was challenging. GC-MS analysis showed that two products, in addition to 3A5AF, were present with retention times of 4.876 min (*m/z* 165.1 g/mol), the major product and 5.086 min (*m/z* 183.1 g/mol). The latter could be assigned to product **1** or **1'** based on their mass and the former to **2** as proposed in Scheme 3 (or an imine that would form via dehydration of **1'**). Dehydration would be favoured in these reactions as it results in the formation of a multiple bond conjugated with the furan ring. As **1** and **1'** are isomers, the reaction work-up was varied in order to determine which products had formed. In the presence of acid, the peak assigned to **1** at retention time 5.086 min disappeared and the peak for **2** at 4.876 min grew in intensity – indicating that an acid catalysed dehydration had occurred. However, upon further aqueous work up in the presence of aqueous sodium bicarbonate solution to quench excess acid, the peak for **2** disappeared and a single product peak for **1** was observed in the GC trace. It should be noted that in a Grignard reaction of another acetyl-substituted aromatic secondary amide, *N*-(4-acetyl-3-methoxyphenyl)-acetamide, either the tertiary alcohol or hemiaminol product could be isolated depending on the exact nature of the reaction conditions employed.[24]

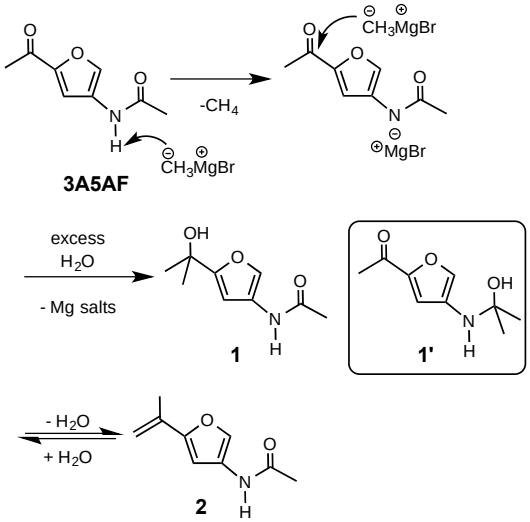

Scheme 3. Reaction of 3A5AF and CH_3MgBr to yield amido-alcohol (**1**) and alkene (**2**) products. Alternative product (**1'**), an isomer of 1, inset bottom right.

The IR spectrum of the reaction mixture was compared with that of pure 3A5AF. As there was still some unreacted 3A5AF in the mixture, conclusions regarding changes of $\nu_{C=O}$ could not be made. Furthermore, the generation of the alkenyl C=C bond in **2** could not be confirmed because the range of $\nu_{C=C}$ would overlap with the aromatic $\nu_{C=C}$ of the furan ring. However, the IR ν_{C-H} bands of the methyl groups have increased in intensity for the reaction mixture (2920 – 2978 cm^{-1}), confirming addition of the methyl group.

In addition to IR and mass spectrometric analysis, NMR spectra of possible products were predicted computationally, and were compared with the experimental results. In the experimental ^{13}C NMR spectra, a peak at 167.4 ppm was assigned to δ(CO) in the product **1** (Scheme 3). The predicted δ(CO) occurs at a higher frequency (176.0 ppm) but was acceptably in accordance with the experimental data. The alcoholic quaternary C atom in **1** has a predicted chemical shift of 74.9 ppm (cf. 67.8 ppm experimentally) and is located in a unique position within the ^{13}C NMR spectrum compared with the predicted spectra of **1**'. This strongly suggests that the product of the Grignard reaction is a tertiary alcohol. Although, ^{13}C NMR spectroscopy, both experimental and computational, has aided in identifying **1** - it cannot be relied on alone to unequivocally identify the reaction products.

3. Conclusions

3-acetamido-5-acetylfuran is a recently developed renewable compound that can be obtained from *N*-acetyl-D-glucosamine, the monomer of chitin. Several physical and chemical properties of 3A5AF were studied by both computational and experimental work. The experimental pK_a value of 3A5AF was obtained as 20.7 ± 0.1 through UV-Vis titration, which was consistent with the theoretical prediction of a pK_a in the range 18.5 - 21.5. 3A5AF is soluble in $scCO_2$ with methanol as a co-solvent, but could not dissolve directly in neat $scCO_2$ within the temperature and pressure ranges tested. Compared with some other chemicals from biomass such as 5-HMF, the solubility of 3A5AF in $scCO_2$ is low. A possible reason is that stronger solute-solute interactions exist between 3A5AF molecules such as intermolecular hydrogen-bonding between the acetyl and amide groups. The computed dimerization energies provided further evidence that 3A5AF can form dimers more easily than 5-HMF. The frequency of the C=O stretching band for 3A5AF neat was lower than that in solution, indicating stronger intermolecular forces (hydrogen-bonding) exist in the solid state. In ^1H NMR spectra, samples with higher concentrations exhibited less temperature dependent variation in δ(NH). These results show that hydrogen-bonding exists between 3A5AF molecules in solution, and is stronger in higher concentration samples. Furthermore, the rate of deuterium exchange in more concentrated samples was slower than in dilute samples. The frontier orbitals and ESP charges of 3A5AF were determined. A Grignard reaction of 3A5AF with CH_3MgBr was performed. 3A5AF was found to be less reactive than acetophenone under similar conditions and a tertiary alcohol product (**1**) formed that was susceptible to acid-catalysed dehydration. As 3A5AF is still a relatively new compound, which has not been studied extensively, these studies will be helpful in designing future reactions and processes involving this molecule.

Experimental Section

Computational Details

All calculations were carried out using Gaussian 09.[25] Each structure was first optimized using the B3LYP functional and the 6-311+G(2d,p) basis set.[16] For the calculation of the pK_a, the gas phase Gibbs energies were calculated using the G3MP2[15] method to obtain greater accuracy. The solvation energies were calculated using the Polarizable Continuum Model (PCM)[26] for DMSO and B3LYP/6-311+G(2d,p) method. In the dimerization energy calculations, molecular energies were calculated for 3A5AF and 5-HMF molecules using the B3LYP/6-311+G(2d,p) method. A counterpoise correction was performed in the interaction energy calculation.[27] The TD-DFT excitation energies, ESP charges, electrostatic potential surfaces, and molecular orbitals were calculated using B3LYP/6-311+G(2d,p). The predicted NMR spectra were calculated using the PCM for chloroform as the solvent and B3LYP/6-311+G(2d,p) method.

pK_a Measurement

DMSO was dried with calcium hydride and distilled prior to use. All glassware was oven-dried. The potassium dimsyl solution was prepared in a glovebox by adding around 40 mg potassium hydride to 10.00 mL DMSO slowly with stirring. The solution obtained was pale yellow, and turned pink after the addition of one drop of triphenylmethane solution (1.3 mg dissolved in several drops of DMSO) to stabilize the solution. The accurate concentration of the potassium dimsyl solution was measured internally in the first stage of the titration. 103.7 mg fluorene was added to 12.00 mL DMSO to form a 51.99 mmol/L indicator solution. 3A5AF was synthesized using a literature procedure,[4] extracted from the reaction mixture using ethyl acetate (EtOAc, ACS grade), purified using flash chromatography, and dried overnight under vacuum using a Schlenk line. 48.9 mg 3A5AF was dissolved in 6.00 mL DMSO to form a 48.8 mmol/L solution.

The titration process followed the work of Bordwell and co-workers,[17b] using an Ocean Optics USB4000-UV-Vis spectrometer. As part of the absorption band of the fluorenide anion (400 – 600 nm) overlaps with sections of the absorption bands of the 3A5AF molecule and its anion (300 – 700 nm), a wavelength for the calculation outside of this region was used. In a DMSO solution of 3A5AF, the extinction coefficient of 3A5AF molecule, ε_1, was calculated using Beer's law at wavelength λ_1. In the ionized 3A5AF solution in potassium dimsyl, the concentration of 3A5AF molecules could be calculated from the absorbance at λ_1, thus allowing the concentration of 3A5AF anions to be calculated. λ_2 in the region of the 3A5AF anion absorption was chosen so it did not overlap with the region of the 3A5AF molecular absorption, allowing the extinction coefficient for the 3A5AF anion, ε_2, to be obtained. Therefore, in the titration process, the changes in absorption intensity at λ_2 could be recorded and used for calculating the 3A5AF anion concentration. UV-Vis spectra are provided in the Supporting Information.

Solubility in $scCO_2$

A SFT-Phase Monitor II instrument (Supercritical Fluid Technologies Inc.) was used to adjust temperatures and pressures, and record cloud points for mixtures. The view cell was 30 mL in volume. In the first test, solubility in neat $scCO_2$, 17.5 mg solid 3A5AF was placed directly into the cell. In the second test, 13.0 mg 3A5AF was dissolved in 3.00 mL methanol (HPLC grade), then the solution was injected into the cell. Cloud point data were obtained using a previously reported experimental procedure (including pressurization and equilibration steps).[18] A video of a phase change for 3A5AF in $scCO_2$/methanol at 50 °C is available in the Supporting Information.

Infrared Measurement

A Bruker Alpha FT-IR spectrometer was used. 3A5AF and 5-HMF solid, a 4.88 mmol/L 3A5AF in Et_2O solution and a 5.15 mmol/L 5-HMF in

Et_2O solution were measured. IR spectra are available in the Supporting Information.

NMR Measurement for the Hydrogen-bonding Experiments

29.4 mg 3A5AF was dissolved in 4.00 mL $CDCl_3$ to give a 7.35 mg/mL solution. 1.00 mL was withdrawn and diluted with 2.00 mL $CDCl_3$, from which 1.00 mL was taken and mixed with 2.00 mL $CDCl_3$. Thus the 2.45 mg/mL and 1.23 mg/mL solutions were prepared. On a Bruker AVANCE III NMR 300, ^1H NMR spectra were obtained for the three samples at 298 K and 323 K. Then approximately one equivalent of D_2O was added to the three solutions. After being shaken and left for 10 minutes, the samples were run again to observe the exchange of the proton in the amide group with the deuterium in D_2O.

Reaction of 3A5AF with CH_3MgBr

3A5AF (51.4 mg, 0.307 mmol) was dissolved in dry tetrahydrofuran (THF) and transferred to a Schlenk flask. The solvent was evaporated under vacuum. Under N_2 flow, dry THF (ca. 8 mL) was added to the Schlenk flask to dissolve the solid. The flask was cooled in an ice bath and 0.26 mL (0.78 mmol) CH_3MgBr solution (3.0 M, in Et_2O) was added with stirring. The ice bath was removed and the mixture was stirred under N_2 at room temperature for 1 h. Deionized water (ca. 10 mL) was added to the brown cloudy mixture. The mixture was stirred for 30 min. THF was removed under vacuum, and EtOAc (5 × ca. 3 mL) was added to extract the products. An aliquot of the combined EtOAc extracts was injected into GC-MS for analysis. EtOAc was removed under vacuum from the combined extracts and the resulting solid was dissolved in $CDCl_3$ for ^1H and ^{13}C NMR analysis. GC-MS and NMR spectra are provided in the Supporting Information. This reaction was repeated with both (i) acidic work-up (a few drops of $HCl_{(aq)}$ were added during the reaction quenching step) and (ii) acidic/basic work-up (same as (i) but aqueous sodium bicarbonate was added prior to extraction with EtOAc).

Acknowledgements

We thank Memorial University, NSERC of Canada, Research & Development Corporation Newfoundland and Labrador, Canada Foundation for Innovation and the Hebron project (Diversity fund) for generous funding. Calculations were performed using the ACEnet consortium of Compute Canada.

Keywords: renewable resources· acidity · solubility · DFT study · hydrogen bonds

[1] a) D. M. Alonso, J. Q. Bond, J. A. Dumesic, *Green Chem.* **2010**, *12*, 1493-1513; b) J. J. Bozell, G. R. Petersen, *Green Chem.* **2010**, *12*, 539-554; c) P. Gallezot, *Chem. Soc. Rev.* **2012**, *41*, 1538-1558; d) H. Kobayashi, A. Fukuoka, *Green Chem.* **2013**, *15*, 1740-1763; e) L. E. Manzer, *Top. Catal.* **2010**, *53*, 1193-1196; f) R. A. Sheldon, *Green Chem.* **2014**; g) J.-L. Wertz, and O. Bédué, *Lignocellulosic Biorefineries*, EFPL Press, [N.p.], **2013**.

[2] a) T. Buntara, S. Noel, P. H. Phua, I. Melian-Cabrera, J. G. de Vries, H. J. Heeres, *Angew Chem Int Ed Engl* **2011**, *50*, 7083-7087; b) T. M. Lammens, M. C. R. Franssen, E. L. Scott, J. P. M. Sanders, *Green Chem.* **2010**, *12*, 1430-1436.

[3] a) M. Rinaudo, *Prog. Polym. Sci.* **2006**, *31*, 603-632; b) F. M. Kerton, Y. Liu, K. W. Omari, K. Hawboldt, *Green Chem.* **2013**, *15*, 860-871.

[4] K. W. Omari, L. Dodot, F. M. Kerton, *ChemSusChem* **2012**, *5*, 1767-1772.

[5] a) R. A. Franich, S. J. Goodin, A. L. Wilkins, *J. Anal. Appl. Pyrolysis* **1984**, *7*, 91-100; b) J. Chen, M. Wang, C.-T. Ho, *J. Agric. Food. Chem.* **1998**, *46*, 3207-3209.

[6] M. W. Drover, K. W. Omari, J. N. Murphy, F. M. Kerton, *RSC Adv.* **2012**, *2*, 4642-4644.

[7] X. Chen, S. L. Chew, F. M. Kerton, N. Yan, *Green Chem.* **2014**, *16*, 2204-2212.

[8] M. Osada, K. Kikuta, K. Yoshida, K. Totani, M. Ogata, T. Usui, *Green Chem.* **2013**, *15*, 2960-2966.

[9] Y. Ohmi, S. Nishimura, K. Ebitani, *ChemSusChem* **2013**, *6*, 2259-2262.

[10] a) K. Jackson, S. K. Jaffar, R. S. Paton, *Ann. Rep. Prog. Chem., Sect. B: Org. Chem.* **2013**, *109*, 235-255; b) D. J. Tantillo, *Nat. Prod. Rep.* **2013**, *30*, 1079-1086; c) J. P. Bardhan, *Comput. Sci. Disc.* **2012**, *5*, 013001.

[11] a) F. G. Bordwell, *Acc. Chem. Res.* **1988**, *21*, 456-463; b) K. Iutsu, *Acid-Base Dissociation Constants in Dipolar Aprotic Solvents*, Blackwell Scientific Publications, Oxford, **1990**.

[12] a) D. Gao, P. Svoronos, P. K. Wong, D. Maddalena, J. Hwang, H. Walker, *J. Phys. Chem. A* **2005**, *109*, 10776-10785; b) J. H. Jensen, H. Li, A. D. Robertson, P. A. Molina, *J. Phys. Chem. A* **2005**, *109*, 6634-6643; c) S. Gangarapu, A. T. Marcelis, H. Zuilhof, *ChemPhysChem* **2013**, *14*, 990-995; d) N. Sadlej-Sosnowska, *Theor. Chem. Acc.* **2007**, *118*, 281-293.

[13] a) V. S. Bryantsev, M. S. Diallo, W. A. Goddard, *J. Phys. Chem. A* **2007**, *111*, 4422-4430; b) T. Matsui, T. Baba, K. Kamiya, Y. Shigeta, *PCCP* **2012**, *14*, 4181-4187; c) Z. X. Wong, H. H. Abdallah, *Acta Chim. Slovenica* **2012**, *59*; d) J. Ho, M. L. Coote, *J. Chem. Theory Comput.* **2009**, *5*, 295-306.

[14] a) C. Lim, D. Bashford, M. Karplus, *J. Phys. Chem.* **1991**, *95*, 5610-5620; b) M. D. Liptak, G. C. Shields, *J. Am. Chem. Soc.* **2001**, *123*, 7314-7319.

[15] L. A. Curtiss, P. C. Redfern, K. Raghavachari, V. Rassolov, J. A. Pople, *J. Chem. Phys.* **1999**, *110*, 4703-4709.

[16] a) K. Raghavachari, G. W. Trucks, *J. Chem. Phys.* **1989**, *91*, 1062-1065; b) A. D. Becke, *Phys. Rev. A* **1988**, *38*, 3098-3100; c) C. Lee, W. Yang, R. G. Parr, *Phys. Rev. B* **1988**, *37*, 785-789; d) S. H. Vosko, L. Wilk, M. Nusair, *Can. J. Phys.* **1980**, *58*, 1200-1211.

[17] a) Y. Chu, H. Deng, J.-P. Cheng, *J. Org. Chem.* **2007**, *72*, 7790-7793; b) W. S. Matthews, J. E. Bares, J. E. Bartmess, F. Bordwell, F. J. Cornforth, G. E. Drucker, Z. Margolin, R. J. McCallum, G. J. McCollum, N. R. Vanier, *J. Am. Chem. Soc.* **1975**, *97*, 7006-7014.

[18] S. M. Payne, F. M. Kerton, *Green Chem.* **2010**, *12*, 1648-1653.

[19] V. K. Potluri, J. Xu, R. Enick, E. Beckman, A. D. Hamilton, *Org. Lett.* **2002**, *4*, 2333-2335.

[20] F. M. Kerton, *Alternative Solvents for Green Chemistry*, RSC Publishing, Cambridge,, **2013**, pp. 115-148.

[21] B. Hakkarainen, K. Fujita, S. Immel, L. Kennea, C. Sandström, *Carbohydr. Res.* **2005**, *340*, 1539-1545.

[22] C. J. Cramer, *Essentials of computational chemistry: theories and models*, John Wiley & Sons, **2013**.

[23] a) P. Politzer, J. S. Murray, *Fluid Phase Equilib.* **2001**, *185*, 129-137; b) J. S. Murray, P. Politzer, *THEOCHEM* **1998**, *425*, 107-114.

[24] C. A. Broka, D. S. Carter, M. P. Dillon, R. C. Hawley, A. Jahangir, C. J. J. Lin*, et al.*, "Preparation of diaminopyrimidines as P2X3 and P2X2/3 antagonists," US20050209260A1, 2005

[25] M. J. Frisch, G. W. Trucks, H. B. Schlegel, G. E. Scuseria, M. A. Robb, J. R. Cheeseman, G. Scalmani, V. Barone, B. Mennucci, G. A. Petersson, H. Nakatsuji, M. Caricato, X. Li, H. P. Hratchian, A. F. Izmaylov, J. Bloino, G. Zheng, J. L. Sonnenberg, M. Hada, M. Ehara, K. Toyota, R. Fukuda, J. Hasegawa, M. Ishida, T. Nakajima, Y. Honda, O. Kitao, H. Nakai, T. Vreven, J. A. Montgomery, J. E. P. Jr., F. Ogliaro, M. Bearpark, J. J. Heyd, E. Brothers, K. N. Kudin, V. N. Staroverov, R. Kobayashi, J. Normand, K. Raghavachari, A. Rendell, J. C. Burant, S. S. Iyengar, J. Tomasi, M. Cossi, N. Rega, J. M. Millam, M. Klene, J. E. Knox, J. B. Cross, V. Bakken, C. Adamo, J. Jaramillo, R. Gomperts, R. E. Stratmann, O. Yazyev, A. J. Austin, R. Cammi, C. Pomelli, J. W. Ochterski, R. L. Martin, K. Morokuma, V. G. Zakrzewski, G. A. Voth, P. Salvador, J. J. Dannenberg, S. Dapprich, A. D. Daniels, Ö. Farkas, J. B. Foresman, J. V. Ortiz, J. Cioslowski, D. J. Fox, Gaussian, Inc., Wallingford, CT, **2009**.

[26] a) J. Tomasi, B. Mennucci, R. Cammi, *Chem. Rev.* **2005**, *105*, 2999-3094; b) M. Cossi, N. Rega, G. Scalmani, V. Barone, *J. Comput. Chem.* **2003**, *24*, 669-681.

[27] S. F. Boys, F. Bernardi, *Mol. Phys.* **1970**, *19*, 553-566.

Received: ((will be filled in by the editorial staff))
Published online: ((will be filled in by the editorial staff))

Entry for the Table of Contents

ARTICLES

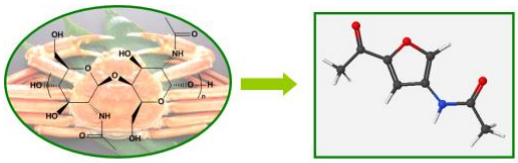

Properties of a renewable furyl-amide: 3-acetamido-5-acetylfuran (3A5AF) can be made from *N*-acetyl-D-glucosamine (NAG), the monomer of chitin, present in shellfish waste (see picture). 3A5AF might be a future building block for amines and N-containing polymers but little is known about it at present. In this paper, the pK_a, solubility and hydrogen-bonding of this molecule are discussed.

Yi Liu, Prof. Christopher N. Rowley and Prof. Francesca M. Kerton**

Page No. – Page No.

Combined experimental and computational studies on the physical and chemical properties of the renewable amide, 3-acetamido-5-acetylfuran